Bioorganic & Medicinal Chemistry 20 (2012) 3596–3602

Contents lists available at SciVerse ScienceDirect

Bioorganic & Medicinal Chemistry

journal homepage: www.elsevier.com/locate/bmc

Inverse Virtual Screening allows the discovery of the biological activity of natural compounds

Gianluigi Lauro, Milena Masullo, Sonia Piacente, Raffaele Riccio, Giuseppe Bifulco *

Dipartimento di Scienze Farmaceutiche e Biomediche, Università di Salerno, Via Ponte Don Melillo, 84084 Fisciano (SA), Italy

ARTICLE INFO

Article history:
Received 2 February 2012
Revised 26 March 2012
Accepted 30 March 2012
Available online 6 April 2012

Keywords:
Inverse Virtual Screening
Docking
Natural compounds

ABSTRACT

A small library of phenolic natural compounds belonging to different chemical classes was screened on a panel of targets involved in the genesis and progression of cancer. The re-investigation of their potential activity was achieved through the Inverse Virtual Screening approach. The normalization of the predicted binding energies permitted the selection of promising compounds on definite targets, avoiding the selection of false positive results. In vitro biological tests revealed the inhibitory activity of xanthohumol and isoxanthohumol on PDK1 and PKC protein kinases. This study validates the robustness of the Inverse Virtual Screening in silico approach as a useful tool for the identification of the specific biological activity of a given set of compounds.

1. Introduction

The identification of the biological targets of a natural and synthetic compound represents a fundamental aim in medicinal chemistry and in the field of natural products. The discovery of the activity of a molecule on a specific target and a careful analysis at a molecular level of the main interactions can be used to rationalize its binding mode. In this context, computational chemistry represents today a valid and fast tool for the scientific research of new compounds with potential pharmacological activity. It is possible to analyse a large number of molecules in very short times, evaluating their binding mode with receptors of pharmacological interest (Virtual Screening[1]). The availability of the crystallographic structures of specific targets permits the evaluation of the binding mode of specific compounds before the synthesis, with a reduction of costs and timing of a drug discovery project. Nevertheless, there are only few examples where the calculations are performed on different targets characterized by their involvement in specific disease processes. This new type of computational approach is known as Inverse Virtual Screening,[2–5] in which libraries of compounds are tested on a panel of targets with the aim of identifying a specific pharmacological activity (panel of antitumor, antiviral and antibacterial targets). This in silico tool could allow the identification of new specific biological actions for ligands with a well-known activity and explain in some cases the selectivity or the presence of side effects of a compound.[6,7] In particular, the building of the panel of proteins represents a critical step, because the targets must be carefully chosen (choice of subunities and evaluation of the action mechanisms). While the Inverse Virtual Screening approach is conceptually simple, difficulties arise from the analysis of the results. In this regard, we have recently developed a new method of evaluation and selection of the best results applying a normalization of the energy values.[8] This approach was in the first place confirmed by the selection of the topoisomerase I target for two camptothecins,[8] actually able to interact with this target. More recently, we have successfully used this method for the identification of the activity and selectivity of a cyclic peptide named namalide.[9] The specific inhibitory property of this compound on the carboxypeptidase A isoform and the lack of the activity on the U isoform were shown. These data were in perfect agreement with the biological tests and contributed to a validation of this computational protocol.[9] Starting from these encouraging results, we here propose an application of the Inverse Virtual Screening on a small set of phenolic natural compounds tested on a panel of 163 targets involved in the cancer processes. The small library of molecules used in this study consists of 10 compounds with a certain variability of the scaffolds (Table 1) and includes compounds extracted from various plants and widely examined for their different pharmacological actions. The biological properties of these compounds were recognized and their involvement in metabolic disorders,[10] oxidative damage events,[11] atherosclerosis[12] and also in cancer prevention[13–15] was largely demonstrated. The bioactivity of several of these compounds was noteworthy and in some cases the specific targets of interactions were already known. Moreover, the complexity of the pharmacological activity of a given compound could be often explained considering its capacity of interacting with more than one target.

* Corresponding author. Tel.: +39 089969741; fax: +39 089969602.
E-mail address: bifulco@unisa.it (G. Bifulco).

0968-0896/$ - see front matter © 2012 Elsevier Ltd. All rights reserved.
http://dx.doi.org/10.1016/j.bmc.2012.03.072

Table 1
The library of 10 natural compounds used for the screening

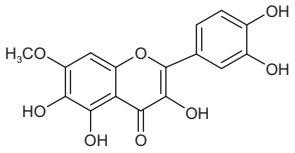

1. 7-*O*-methylquercetagetin

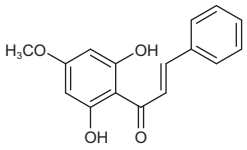

2. 2',6'-dihydroxy-4'-methoxychalcone

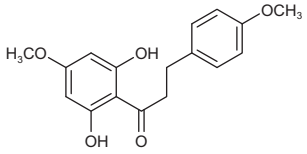

3. 2',6'-dihydroxy-4',4-dimethoxydihydrochalcone

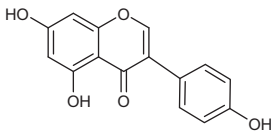

4. genistein

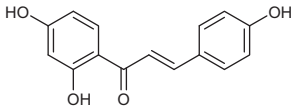

5. isoliquiritigenin

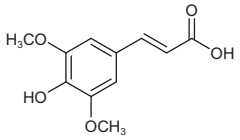

6. sinapic acid

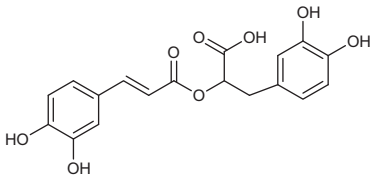

7. rosmarinic acid

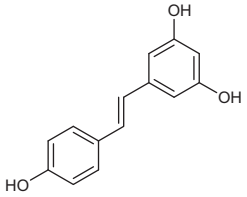

8. resveratrol

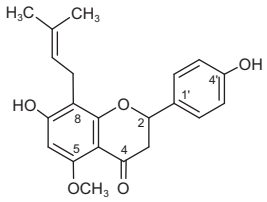

9. isoxanthohumol

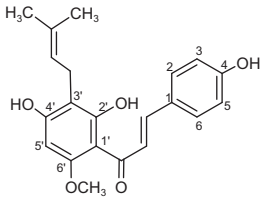

10. xanthohumol

The chemopreventive activity of most of the compounds featuring these scaffolds was largely investigated and often proven by testing them on several cancer cell lines.[16,17] This capacity was mainly attributed to their well-known antioxidant properties.[18] However, many different actions on several targets involved more directly in the progression of this pathology were also shown.[19–21]

In particular, compounds **2**, **3**, **5** and **10** belong to the class of chalcones, for which antioxidant, chemopreventive, anticancer, anti-inflammatory, antifungal and antibacterial activities are reported.[22] A number of chalcone derivatives have also been found to inhibit several important enzymes in cellular systems, including xanthine oxidase, aldose reductase, haem oxygenase, protein tyrosine kinase, quinine reductase and tyrosinase.[14]

Among chalcone derivatives, the prenylated chalcone xanthohumol (**10**) and its derivative isoxanthohumol (**9**) occurring in the cones of *Humulus lupulus,* have attracted a lot of attention because of their biological activities, among which a broad-spectrum antiinfective activity against several microorganisms.[23] Xanthohumol (**10**) has been shown to inhibit the initiation, promotion and progression stages of carcinogenesis, hence behaving as a potential broad-spectrum chemopreventive agent.[24] Recently, we have demonstrated that xanthohumol decreases the viability of the T98G human malignant glioblastoma cell line. Apoptosis induced by xanthohumol is associated with activation of caspase-3, caspase-9 and PARP cleavage and is mediated by the mitochondrial pathway, as exemplified by mitochondrial depolarization, cytochrome c release and downregulation of the antiapoptotic Bcl-2 protein. Moreover, xanthohumol induces intracellular reactive oxygen species (ROS), which provides a specific environment that results in MAPK-induced cell death.[25]

The small library of selected antioxidative phenolic compounds comprises also sinapic acid (**6**), a cinnamic acid derivative, with anti-anxiety properties,[26] rosmarinic acid (**7**) exerting antiinflammatory, antimutagen, antibacterial and antiviral activities[27] and resveratrol (**8**), the well known natural phytoalexin found in considerable amounts in the skin of grapes. In the past years resveratrol (**8**) has received a lot of attention because of its biological activities, as antimutagenic, antiviral, antiinflammatory and cancer preventing. In particular it is believed that because of its antioxidant properties, resveratrol is responsible for the reduced risk of cardiovascular disease associated with a moderate consumption of red wine.[28,29] Moreover the isoflavone genistein (**4**) showed a topoisomerase[22,30] and tyrosine kinase[31] activity.

By considering the wide spectrum of activity of these compounds, a re-evaluation of their biological properties may further clarify their modulatory activity in the cancer events. On the other hand, the phases of extraction and purification imply small quantities of compounds from natural sources and make complex the performance of biological tests on more than one target. In this context, Inverse Virtual Screening represents a useful tool for the re-evaluation and/or the identification of the specific interactions of the library of compounds considered here.

2. Materials and methods

2.1. Inverse Virtual Screening

We built and processed the chemical structures of the library of compounds with Macromodel 8.5 (Schrödinger, LLC, New York, 2003). Molecular mechanics/dynamics calculations were performed on a 4 × AMD Opteron SixCore 2.4 GHz using Macromodel 8.5 and the OPLS force field. To allow a full exploration of the conformational space, we used the Monte Carlo multiple minimum (MCMM) method (5000 steps). Molecular dynamics simulations were performed at a temperature of 600 K and with a simulation time of 10 ns. A constant dielectric term, mimicking the presence of the solvent, was used in the calculations to reduce artefacts. To identify a possible three-dimensional starting model of each compounds for the subsequent docking calculations, we applied an optimization (Conjugate Gradient, 0.05 Å convergence threshold) of the structures. We built the panel of protein targets by a search of crystallized structures in the Protein Data Bank database (www.rcsb.org, Table S1, Supplementary data). Water molecules were removed, and polar hydrogens were added with Autodock-Tools 1.4.5. Molecular docking calculations were performed using Autodock-Vina32 software (Table S2, Supplementary data) and then the predicted binding energies were normalized (Table S3, Supplementary data). This software uses a scoring function that combines advantages of knowledge-based potentials and empirical scoring functions and the Iterated Local Search global optimizer algorithm implemented with the BFGS method for the local optimization. In this way it satisfies at the same time the requirements of fastness and accuracy for the docking calculations.[32] In the configuration file we specified only the exhaustiveness value to 64 and the coordinate values for the targets, focusing the grids on the sites of presumable pharmacological interest. When it was possible, we used as reference the binding mode of crystallized ligands in PDB files (Table S1, Supplementary data). For all the investigated compounds, all open-chain bonds were treated as active torsional bonds. Autodock-Vina results were analyzed with Autodock Tools 1.4.5.

2.2. Isolation of isoxanthohumol (9) and xanthohumol (10)

Humulus lupulus cones (200 g), purchased from BioPlanta s.a.s., Irsina (MT), Italy (lot n° LTH 1002), were extracted with EtOH (3 × 1.5 L) for 20 days. The solvent was removed under reduced pressure to afford 29 g of crude extract. Part of the extract (2.5 g × two times) was fractionated on Sephadex LH-20 (100 × 5 cm) using MeOH as the mobile phase. Fifty fractions (8 mL) were obtained. Fractions 30–38 (230 mg) were chromatographed by semi-preparative HPLC/UV (injections 4 mg/100 μL) using H_2O/0.1% TFA as eluent A and CH_3CN/0.1% TFA as eluent B for the mobile phase to afford xanthohumol (**10**, 40 mg, t_R 29.8 min, at 98% purity) and isoxanthohumol (**9**, 1.8 mg, t_R 23.5 min, at 97% purity). The elution programme started with a linear gradient of 20% of eluent B to 100% of B in 40 min. The detection wavelength was 254 nm. Compounds **9** and **10** were identified by comparison of their NMR and MS data with those reported in the literature.[33,34]

2.3. IC_{50} determination

The IC_{50} profile of five compounds was determined using PDK1, PKC-α, PKC-θ protein kinases (Proqinase, Germany). IC_{50} values were measured by testing 10 concentrations (1×10^{-4} M to 3×10^{-9} M) of each compound in singlicate. All protein kinases were expressed in Sf9 insect cells or in *Escherichia coli* as recombinant GST-fusion proteins or His-tagged proteins. All kinases were produced from human cDNAs and purified by either GSH-affinity chromatography or immobilized metal. A radiometric protein kinase assay (33PanQinase® Activity Assay) was used for measuring the kinase activity of the three protein kinases. All kinase assays were performed in 96-well FlashPlatesTM from PerkinElmer (Boston, MA, USA) in a 50 μl reaction volume. The reaction cocktail consisted of 20 μl of assay buffer (standard buffer), 5 μl of ATP solution (in H_2O), 5 μl of test compound (in 10% DMSO) and 10 μl of substrate/10 μl of enzyme solution (premixed). The reaction cocktails were incubated at 30 °C for 60 min. The reaction was stopped with 50 μl of 2% (v/v) H_3PO_4, plates were aspirated and washed two times with 200 μl 0.9% (w/v) NaCl. Incorporation of 33Pi was determined with a microplate scintillation counter (Microbeta, Wallac). All assays were performed with a BeckmanCoulter/SAGIAN™ Core System.

3. Results and discussion

Using the Inverse Virtual Screening approach we screened the library of 10 compounds on a panel of 163 targets involved in the cancer progression and collected the results in a matrix (Table S2, Supplementary data). Then we normalized the predicted binding energies, using the Eq. 1 (Table S3, Supplementary data):

$$V = V_0/[(M_L + M_R)/2] \quad (1)$$

where V is the normalized value associated to each compound, V_0 is the value of predicted binding energy obtained from the docking calculation (kcal/mol), M_L is the average binding energy of each ligand (on different targets, kcal/mol), and M_R is the average binding energy associated to each target (on the various ligands, kcal/mol) (Table 2).

It is noteworthy that V is an absolute number. This mathematical manipulation causes the loss of the original significance of the binding energy as a value for the prediction of activity of a given compound. The normalized values can be used to generate a ranking in which the best values represent a promising interaction between a compound and a target from the panel. Moreover, taking into account the average trends in Eq. 1 the selection of false positive results can be avoided.[8] It is important to stress that the main aim of this study is the identification of the targets interacting with a compound. The correspondence between the predicted and the calculated binding energies is much more difficult with respect to a classical Virtual Screening, in which only one target is studied, and mainly for two reasons. First, the comparison of the results for several targets even if normalized reduces but does not completely eliminate the problem of the variability of the interacting binding sites. In the second place, Autodock-Vina is a very fast and accurate software for the docking calculations, but in some cases a sensible deviation from the experimental results could be observed in the prediction of the binding energies. This could depend in a variable way also by the number of active rotatable bonds of the investigated compounds.[32]

The selection of the best results was so conducted sorting and analysing the normalized results of the screening from the best to the worse value. We observed that the best two normalized results highlighted the correlation between isoxanthohumol (**9**) with PKC-α[35] (Protein Kinase C α, V value = 1.286, position nr.1 in the final ranking on 1630 total calculations) and xanthohumol (**10**) with PDK1[36] (phosphoinositide-dependent kinase 1, V value = 1.264, position nr.2 in the final ranking). Moreover, the presence in the panel of the PKC-θ[37] isoform, characterized by a binding site related to PKC-α,[38] prompted us to explore the behavior of isoxanthohumol (**9**) with this target. Interestingly, the normalized result (V = 1.213) is at the significant position number 14. On the other hand the normalized results for **9** indicated a poor value of V for PDK1 (V = 0.982, position number 921).

Table 2
Predicted binding energies (V_0, kcal/mol), M_R and M_L average values for a sample of 10 ligands on 10 targets for the calculations of the V normalized values

	1	**2**	**3**	**4**	**5**	**6**	**7**	**8**	**9**	**10**	M_R
abl	−8.4	−8.5	−9.0	−9.8	−9.1	−6.7	−8.9	−9.1	−7.6	−9.0	−8.6
abl2	−8.3	−8.2	−7.7	−8.3	−8.8	−7.0	−9.8	−8.8	−6.9	−9.1	−8.3
aif	−8.7	−8.6	−8.5	−8.4	−8.7	−6.7	−8.7	−8.2	−9.1	−9.6	−8.5
akt1	−8.5	−8.0	−7.8	−7.8	−8.2	−6.3	−8.3	−7.4	−8.7	−8.3	−7.9
akt2	−8.1	−8.1	−7.6	−8.2	−8.0	−6.4	−8.7	−7.5	−8.6	−7.7	−7.9
alk	−7.4	−6.7	−6.2	−7.7	−7.1	−5.6	−7.2	−6.6	−7.7	−7.5	−7.0
alk5	−8.1	−7.3	−7.7	−8.3	−8.2	−6.4	−8.8	−7.8	−8.5	−8.0	−7.9
ape1	−6.9	−6.4	−6.1	−7.3	−6.9	−5.5	−6.8	−6.8	−7.1	−6.6	−6.6
aurkin	−9.0	−8.0	−8.0	−8.7	−8.4	−6.7	−8.7	−8.5	−9.7	−8.5	−8.4
aurkinB	−7.7	−7.2	−7.1	−7.8	−7.7	−5.7	−7.1	−7.0	−7.8	−7.3	−7.2
Other targets											
M_L	−7.7	−7.2	−7.1	−7.6	−7.5	−5.9	−7.8	−7.1	−7.8	−7.6	

Table 3
V normalized values for **9** and **10** on PDK1, PKC-α and PKC-θ targets

	PDK1	PKC-α	PKC-θ
9	0.982 (921)	1.286 (1)	1.213 (14)
10	1.264 (2)	0.986 (892)	1.038 (563)

On parenthesis are shown the relative positions in the final ranking on the 1630 total calculations.

Table 4
IC_{50} values for **9** and **10** on PDK1, PKC-α and PKC-θ targets

	PDK1	PKC-α	PKC-θ
9	58.7 μM	45.3 μM	31.6 μM
10	6.6 μM	>100 μM	>100 μM

For what concerns **10**, while the normalized value and the related position in the ranking showed a good predicted activity for PDK1, poor results are observable for PKC-α and PKC-θ (positions 892 and 563, respectively). In Table 3 the values of V and the positions in the final ranking for **9** and **10** with PDK1, PKC-α and PKC-θ are reported.

These targets identified from the screening play a fundamental role in the progression of the tumor events,[39–41] and new inhibitors are searched for the development of new anti-cancer agents. For these reasons, in the next phase we validated these preliminary observations with in vitro biological tests (Table 4). In order to validate the efficacy of the screening also negative controls were considered in this phase (**9** on PDK1, **10** on PKC-α and PKC-θ). Regarding the most promising results, we observed that these compounds confirmed our predictions, showing an inhibitory activity in the μM range. In more detail, xanthohumol (**10**) shows a best activity and selectivity on PDK1 (6.6 μM). Moreover, IC_{50} value calculated for **10** on PKC-α and θ isoforms shows no inhibitory activity at concentrations as high as 10^{-4} M and this is in perfect agreement with the normalized results from the screening. Isoxanthohumol (**9**) is active (less than the previous result) and not selective on PKC-α and θ confirming the selection of the related good positioning from the final ranking. Surprisingly a moderate activity of **9** on PDK1 was highlighted, in spite of the low V value (0.982) and of the low position in the ranking (921). It is important to observe that the best V value found is 1.286, and this means that in this case 921 interactions out of 1630 total calculation are found within a restricted difference of V values of 0.304. Firstly, we wondered whether this lack of sensibility of the approach to avoid a false negative result was caused by the normalization of the affinities. In this context, the ranges from the best to the worse value for the normalized binding energies and for the predicted binding energies before the normalization (RangeV and RangeBE, respectively, Eq. 2) were considered:

$$\text{RangeV} = 1.286 - 0.546 = 0.74;$$
$$\text{RangeBE} = -10.7\ \text{kcal/mol} - (-4.2\ \text{kcal/mol}) = -6.5\ \text{kcal/mol} \quad (2)$$

For the interaction of **9** on PDK1, we calculated the deviations of the V value and of the predicted binding energy from the best ones (Eq. 3).

$$\text{DevV}_{9\text{-PDK1}} = V_{\text{best}} - V_{9\text{-PDK1}};\ \text{DevBE}_{9\text{-PDK1}} = \text{BE}_{best} - \text{BE}_{9\text{-PDK1}} \quad (3)$$

where V_{best} and BE_{best} are the best values of V and predicted binding energies for the 1630 total calculations, and $V_{\mathbf{9}\text{-PDK1}}$ and $\text{BE}_{\mathbf{9}\text{-PDK1}}$ are the V and the predicted binding energies values for the interaction of **9** with PDK1.

Then we divided the these two deviations for the two ranges for the two types of calculation (Eq. 4).

$$\text{RatioV}_{\mathbf{9}\text{-PDK1}} = \text{DevV}_{\mathbf{9}\text{-PDK1}}/\text{RangeV};\text{RatioBE}_{\mathbf{9}\text{-PDK1}} = \text{DevBE}_{\mathbf{9}\text{-PDK1}}/\text{RangeBE} \quad (4)$$

These parameters indicated the nearness of the two values for the interaction of **9** with PDK1 to the best ones in the two rankings. We found two very similar values ($\text{RatioV}_{\mathbf{9}\text{-PDK1}} = 0.41$; $\text{RatioBE}_{\mathbf{9}\text{-PDK1}} = 0.40$). We can conclude that this unexpected result strongly depends from the original value of predicted binding energy. Moreover, it is important to note that the evaluation of the binding energies before normalization do not allow the selection of this false negative. Furthermore, we can observe a low value of $\text{DevBE}_{\mathbf{9}\text{-PDK1}}$ that corresponds in an overcrowding of many values better than $\text{BE}_{\mathbf{9}\text{-PDK1}}$ in a restricted range, as we have initially observed for the normalized values. This means that low variations of the values of predicted binding energies may cause large variations in the two final rankings. For these reasons, in an Inverse Virtual Screening study the choice of the parameters that can affect the estimation of the calculated affinities (i.e., the protein preparation, the exhaustiveness values and the grid boxes for Autodock-Vina) is of primary importance. Accordingly, as we have previously demonstrated that in other case studies,[8,9] the normalization could be a useful tool to avoid false positive and negative results.

In order to give further validation to the method, we performed a similar study using another library of 10 compounds able to bind 10 targets in the panel of 163 targets with high efficacy. We chose these compounds considering the availability of the crystallographic structures of the complexes with the partner receptors. Also in this case we obtained a matrix of 1630 calculations and then we normalized them (Tables S4 and S5, Supplementary data). In Table 5 are listed the V values, the positions in the ranking, the experimental and predicted values of IC_{50} for the 10 compounds with their specific targets. For the listed compounds Autodock-Vina found the crystallographic poses with high accuracy (RMSD <2 Å), and so the predicted binding energies could be related to the experimental ones. Also in this case, using the Inverse Virtual

Table 5
V Values, positions in the ranking, the experimental IC_{50} and predicted affinities for the 10 reference compounds with their specific targets

Reference ligands	*V* (positions in the ranking)	Experimental IC_{50}[42]	Predicted affinities (nM)
ABL_lig	1.421 (**4**)	170.0 nM	0.35
ALK5_lig	1.145 (**168**)	72.0 nM	65
CK2_lig	1.446 (**3**)	52.0 nM	5.2
CLK3_lig	1.062 (**451**)	29.2 nM	129
JAK1_lig	1.097 (**304**)	1.6 nM	497
PDK1_lig	1.585 (**1**)	1.0 nM	0.0085
PKC-α_lig	1.230 (**38**)	2.1 nM	6.2
PKC-θ_lig	1.341 (**8**)	na	1.35
RAF_lig	1.495 (**2**)	1.6 nM	0.055
TP_lig	1.115 (**242**)	20.0 nM	1160

Screening approach we can highlight that four right correlations between ligands and targets are found in the first four positions, a fifth is identified, in the first eight positions and a sixth in the first thirty-eight. The remaining four correct correlations are found far from the high rank positions, so resulting as false negative mainly for their lower values of predicted binding energies.

The availability of the ligands crystallized in the binding sites of the targets PDK1, PKC-α and PKC-θ and active in the nM range allowed a more precise comparison with the *V* values calculated for the compounds **9** and **10** emerging from the screening. We built a third matrix for the 163 targets interacting with **9**, **10**, PDK1_lig, PKC-α_lig and PKC-θ_lig (Table S6, Supplementary data). In Table 6 are reported the *V* values for **9** and **10** on the three targets compared with the *V* values of the reference compounds.

In this way a more precise and accurate correspondence between the *V* values and the experimental IC_{50} was found. Above all, these new scale of values also justified the moderate activity of the compounds **9** and **10** on the three kinases.

In summary, while the normalization method could reduce the possibility of selection of false positive and negative results, the comparison with the *V* values of reference compounds could give qualitative indications for the prediction of the range of activity for a given set of compounds. In particular, for compounds **1**–**10**, five predictions of activity on six actually fitted with the biological tests.

Table 6
V values for **9**, **10**, PDK1_lig, PKC-α_lig and PKC-θ_lig on PDK1, PKC-α and PKC-θ targets

	9	**10**	Reference compounds
PDK1	0.898	1.154	1.529
PKC-α	1.147	0.878	1.235
PKC-θ	1.050	0.897	1.291

3.1. Analysis of the docked structures

An accurate analysis of the main interactions of the compounds selected from the screening in the binding sites of the different targets allows an explanation of the different activity and selectivity

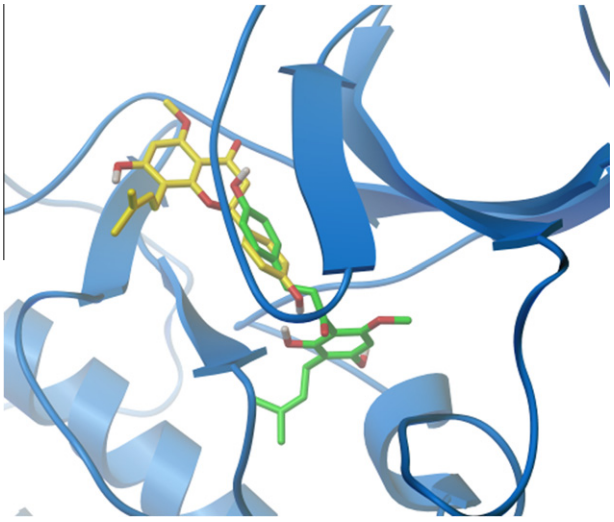

Figure 2. Superimposition between **9** (coloured by atom types: C yellow, H grey, O red) and **10** (coloured by atom types: C green, H grey, O red) in the binding site of PDK1.

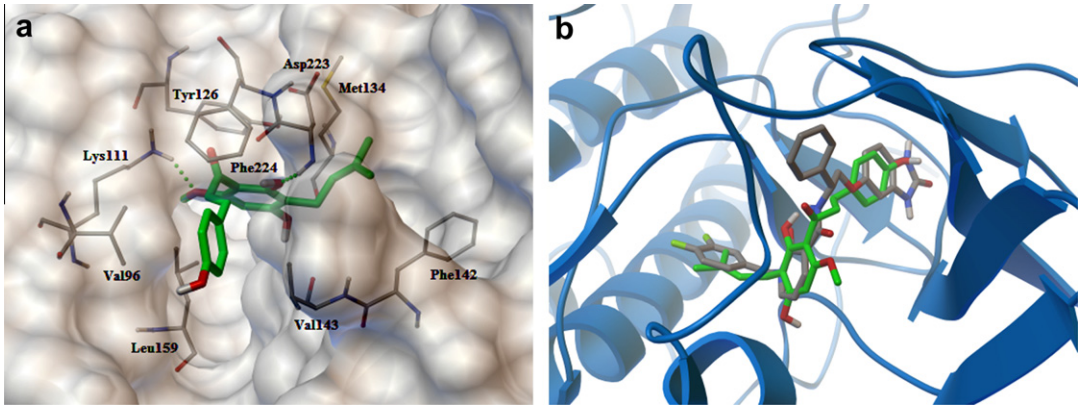

Figure 1. (a) Compound **10** (coloured by atom types: C green, H grey, O red) in docking with PDK1. Hydrogen bonds are displayed with green spheres; (b) superimposition between **10** (coloured by atom types: C green, H grey, O red) and 1-(3,4-difluorobenzyl)-2-oxo-*N*-{(1*R*)-2-[(2-oxo-2,3-dihydro-1*H*-benzimidazol-5-yl)oxy]-1-phenylethyl}-1,2-dihydropyridine-3-carboxamide (coloured by atom types: C dark grey, H grey, O red, N blue) with PDK1.

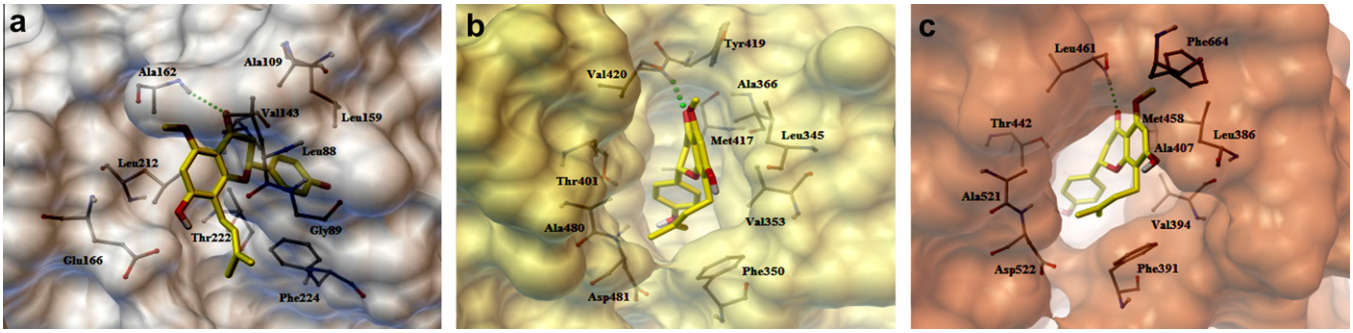

Figure 3. Compound **9** (coloured by atom types: C yellow, H grey, O red) in docking with: (a) PDK1; (b) PKC-α; (c) PKC-θ. Hydrogen bonds are displayed with green spheres.

of the different compounds on the panel of targets used. The best pose from the docking calculations for each compound on the three specific targets was considered in this phase.

Regarding the xanthohumol (**10**) case we observed a very good occupancy of the binding site of PDK1. As illustrated in Figure 1a, **10** is able to establish a set of hydrophobic and electrostatic interactions in the binding pocket composed by Val96, Tyr126, Met134, Phe142, Val143, Leu159 and Phe224. It also involved in two Hydrogen bonds with the nitrogen in the side chain of Lys111 (with the oxygen of the $-OCH_3$ in 6′ position) and with the nitrogen in the backbone of the Asp223 (with the –OH in 2′ position). Moreover, the isopentenyl portion of the compound is accommodated in an internal hydrophobic pocket of PDK1. A good superposition between **10** and 1-(3,4-difluorobenzyl)-2-oxo-*N*-{(1*R*)-2-[(2-oxo-2,3-dihydro-1*H*-benzimidazol-5-yl)oxy]-1-phenylethyl}-1,2-dihydropyridine-3-carboxamide crystallized in the binding site of PDK1[36] could be considered as further confirmation (Fig. 1b). The two phenyl portions of **10** are overlapped with two aromatic portions of the crystallized ligand, respecting their distances and orientations. For what concerns the interactions between isoxanthohumol (**9**) and PDK1, we can primarily observe a most external occupancy of the binding site than the xanthohumol (**10**) and an inversion of the aromatic ring presenting the isopentenyl part that in this case is orientated on the external face of the binding site. The different accommodation of the two compounds and of their pharmacophoric portions in a more deep position of the PDK1 binding site could explain the different activities on this target (Fig. 2).

The binding pocket of PDK1 involved in the interactions with **9** is composed of Leu88, Gly89, Ala109, Val143, Leu159, Glu166, Leu212, Thr222 and Phe224. A hydrogen bond is established between the oxygen of the carbonyl in position 4 of **9** and the nitrogen in the backbone of Ala162 (Fig. 3a).

The analysis of the docked structures of **9** with the PKC (α and θ isoforms) revealed the accommodation of the compound in the binding sites mainly through hydrophobic interactions. In fact, in the case of the α isoform the compound interacts with the following residues: Leu345, Phe350, Val353, Ala366, Thr401, Met417, Tyr419, Val420, Ala480 and Asp481. A hydrogen bond is also observable between the nitrogen in the backbone of Val420 and the oxygen in position 4 of the carbonyl of **9** (Fig. 3b). On the other hand, the best binding pose in the binding site of PKC-θ isoform shows the involvement of a pocket of residues composed of Leu386, Phe391, Val394, Ala407, Thr442, Met458, Ala521, Asp522 and Phe664. Also in this case, a hydrogen bond is established between the nitrogen in the backbone of the Leu461 and the 4-carbonylic oxygen of **9** (Fig. 3c). We considered this theoretical hypothesis of binding modes reliable for two reasons. In the first place. the good result from the biological tests could be considered as an experimental proof of the binding of **9** and **10** in these specific sites of action. Moreover, these compounds show a simple chemical structure mainly characterized by a small number of aromatic rings and of active rotatable bonds.

In these conditions Autodock-Vina software shows a high accuracy of the prediction of the experimental crystallographic poses, with low RMSD values compared to the predicted ones. For these reasons these results could be considered as reasonable models of binding.

4. Conclusions

We have here described the kinase inhibition of two molecules from a small library of natural compounds and validated it through biological tests. A good correlation between the Inverse Virtual Screening results and the biological data, corroborated by 5 prediction of activity/inactivity on 6, was observed.

From a general point of view, Inverse Virtual Screening represents a new computational tool for the identification of targets of pharmacological interest rather than a method for the precise prediction of the range of activity for one or more compounds. Indeed, the normalization of the predicted binding energies considering the average trends of the ligands (on the targets) and of the targets (on the ligands) is useful to identify significant results by a large set of data from heterogeneous sources.

We observed for the compounds identified in this study moderate biological activities. This is in line with the hypothesis of a modulatory role of these molecules in the cancer events. Moreover, the μM range of activity is fully compatible with the role of cancer prevention that is achievable by a consistent exposure to non-toxic agent (i.e., food product).[43]

Using this method, it is possible to obtain a restricted set of receptors related to each compound, focusing the biological tests on a small set of targets. In this way it is possible to achieve results in fast times: using a server equipped with a 4 × AMD Opteron SixCore the total time of calculations and analysis of the total 1630 results is about 15 days. On the other hand, it makes possible the discovery of new molecular scaffolds on a specific receptor as lead compounds and suggested a possible improvement of their potency and selectivity focused on a precise and defined biological context. In particular, precise modifications in the pharmacophore models of these compounds could increase their inhibition on the kinases selected from the screening preserving at the same time their antioxidant and chemopreventive activities. These results highlight the applicability and reliability of this new computational tool.

Acknowledgments

Financial support was provided by the University of Salerno and by Ministero dell'Istruzione, dell'Università e della Ricerca (MIUR),

PRIN 2009 'Design, conformational and configurational analysis of novel molecular platforms' .

Supplementary data

Supplementary data associated with this article can be found, in the online version, at http://dx.doi.org/10.1016/j.bmc.2012.03.072.

References and notes

1. Rester, U. *Curr. Opin. Drug Disc. Dev.* **2008**, *11*, 559.
2. Chen, Y. Z.; Zhi, D. G. *Proteins Struct. Funct. Genet.* **2001**, *43*, 217.
3. Hui-Fang, L.; Qing, S.; Jian, Z.; Wei, F. *J. Mol. Graphics Modell.* **2010**, *29*, 326.
4. Li, H.; Gao, Z.; Kang, L.; Zhang, H.; Yang, K.; Yu, K.; Luo, X.; Zhu, W.; Chen, K.; Shen, J.; Wang, X.; Jiang, H. *Nucleic Acids Res.* **2006**, *34*, 219.
5. Zahler, S.; Tietze, S.; Totzke, F.; Kubbutat, M.; Meijer, L.; Vollmar, A. M.; Apostolakis, J. *Chem. Biol.* **2007**, *14*, 1207.
6. Keiser, M. J.; Setola, V.; Irwin, J. J.; Laggner, C.; Abbas, A. I.; Hufeisen, S. J.; Jensen, N. H.; Kuijer, M. B.; Matos, R. C.; Tran, T. B.; Whaley, R.; Glennon, R. A.; Hert, J.; Thomas, K. L. H.; Edwards, D. D.; Shoichet, B. K.; Roth, B. L. *Nature* **2009**, *462*, 175.
7. Mestres, J.; Seifert, S. A.; Oprea, T. I. *Clin. Pharmacol. Ther.* **2011**, *90*, 662.
8. Lauro, G.; Romano, A.; Riccio, R.; Bifulco, G. *J. Nat. Prod.* **2011**, *74*, 1401.
9. Cheruku, P.; Plaza, A.; Lauro, G.; Keffer, J.; Lloyd, J. R.; Bifulco, G.; Bewley, C. A. *J. Med. Chem.* **2012**, *55*, 735.
10. Mulvihill, E. E.; Allister, E. M.; Sutherland, B. G.; Telford, D. E.; Sawyez, C. G.; Edwards, J. Y.; Markle, J. M.; Hegele, R. A.; Huff, M. W. *Diabetes* **2009**, *58*, 2198.
11. Soobrattee, M. A.; Neergheen, V. S.; Luximon-Ramma, A.; Aruoma, O. I.; Bahorun, T. *Mutat. Res. Fundam. Mol. Mech. Mutagen.* **2005**, *579*, 200.
12. Fan, E.; Zhang, L.; Jiang, S.; Bai, Y. *J. Med. Food* **2008**, *11*, 610.
13. Shankar, S.; Singh, G.; Srivastava, R. K. *Front Biosci.* **2007**, *12*, 4839.
14. Gerhauser, C.; Alt, A. P.; Klimo, K.; Knauft, J.; Frank, N.; Becker, H. *Phytochem. Rev.* **2003**, *1*, 369.
15. Cuendet, M.; Guo, J.; Luo, Y.; Chen, S.; Oteham, C. P.; Moon, R. C.; van Breemen, R. B.; Marler, L. E.; Pezzuto, J. M. *Cancer. Prev. Res. (Phila)* **2010**, *3*, 221.
16. Gerhauser, C.; Alt, A.; Heiss, E.; Gamal-Eldeen, A.; Klimo, K.; Knauft, J.; Neumann, I.; Scherf, H. R.; Frank, N.; Bartsch, H.; Becker, H. *Mol. Cancer Ther.* **2002**, *1*, 959.
17. Shon, Y. H.; Park, S. D.; Nam, K. S. *J. Biochem. Mol. Biol.* **2006**, *39*, 448.
18. Qian, Y. P.; Cai, Y. J.; Fan, G. J.; Wei, Q. Y.; Yang, J.; Zheng, L. F.; Li, X. Z.; Fang, J. G.; Zhou, B. *J. Med. Chem.* **2009**, *52*, 1963.
19. Roy, P.; Kalra, N.; Prasad, S.; George, J.; Shukla, Y. *Pharm. Res.* **2009**, *26*, 211.
20. Hsu, Y. L.; Chia, C. C.; Chen, P. J.; Huang, S. E.; Huang, S. C.; Kuo, P. L. *Mol. Nutr. Food Res.* **2009**, *53*, 826.
21. Deeb, D.; Gao, X.; Jiang, H.; Arbab, A. S.; Dulchavsky, S. A.; Gautam, S. C. *Anticancer Res.* **2010**, *30*, 3333.
22. Sonmez, F.; Sevmezler, S.; Atahan, A.; Ceylan, M.; Demir, D.; Gencer, N.; Arslan, O.; Kucukislamoglu, M. *Bioorg. Med. Chem. Lett.* **2011**, *21*, 7479.
23. Zanoli, P.; Zavatti, M. *J. Ethnopharmacol.* **2008**, *116*, 383.
24. Gerhauser, C. *Eur. J. Cancer* **2005**, *41*, 1941.
25. Festa, M.; Capasso, A.; D'Acunto, C. W.; Masullo, M.; Rossi, A. G.; Pizza, C.; Piacente, S. *J. Nat. Prod.* **2011**, *74*, 2505.
26. Sharma, P. *J. Chem. Pharm. Res.* **2011**, *3*, 403.
27. Petersen, M.; Simmonds, M. S. J. *Phytochemistry* **2003**, *62*, 121.
28. Akiyama, T.; Ishida, J.; Nakagawa, S.; Ogawara, H.; Watanabe, S.; Itoh, N.; Shibuya, M.; Fukami, Y. *J. Biol. Chem.* **1987**, *262*, 5592.
29. Piacente, S.; Montoro, P.; Oleszek, W.; Pizza, C. *J. Nat. Prod.* **2004**, *67*, 882.
30. Okura, A.; Arakawa, H.; Oka, H.; Yoshinari, T.; Monden, Y. *Biochem. Biophys. Res. Commun.* **1988**, *157*, 183.
31. Zhou, N.; Yan, Y.; Li, W.; Wang, Y.; Zheng, L.; Han, S.; Yan, Y.; Li, Y. *Int. J. Mol. Sci.* **2009**, *10*, 3255.
32. Trott, O.; Olson, A. J. *J. Comput. Chem.* **2010**, *31*, 455.
33. Stevens, J. F.; Ivancic, M.; Hsu, V.; Deinzer, M. L. *Phytochemistry* **1997**, *44*, 1575.
34. Tabata, N.; Ito, M.; Tomoda, H.; Omura, S. *Phytochemistry* **1997**, *46*, 683.
35. Wagner, J.; Matt, P. V.; Sedrani, R.; Albert, R.; Cooke, N.; Ehrhardt, C.; Geiser, M.; Rummel, G.; Stark, W.; Strauss, A.; Cowan-Jacob, S. W.; Beerli, C.; Weckbecker, G.; Evenou, J. P.; Zenke, G.; Cottens, S. *J. Med. Chem.* **2009**, *52*, 6193.
36. Nagashima, K.; Shumway, S. D.; Sathyanarayanan, S.; Chen, A. H.; Dolinski, B.; Xu, Y.; Keilhack, H.; Nguyen, T.; Wiznerowicz, M.; Li, L.; Lutterbach, B. A.; Chi, A.; Paweletz, C.; Allison, T.; Yan, Y.; Munshi, S. K.; Klippel, A.; Kraus, M.; Bobkova, E. V.; Deshmukh, S.; Xu, Z.; Mueller, U.; Szewczak, A. A.; Pan, B.; Richon, V.; Pollock, R.; Blume-Jensen, P.; Northrup, A.; Andersen, J. N. *J. Biol. Chem.* **2011**, *286*, 6433.
37. Stark, W.; Bitsch, F.; Berner, A.; Buelens, F.; Graff, P.; Depersin, H.; Fendrich, G.; Geiser, M.; Knecht, R.; Rahuel, J.; Rummel, G.; Schlaeppi, J. M.; Schmitz, R.; Strauss, A.; Wagner, J., www.rcsb.org, PDB code: 2JED.
38. Mellor, H.; Parker, P. J. *Biochem. J.* **1998**, *332*, 281.
39. Peifer, C.; Alessi, D. R. *Biochem. J.* **2009**, *417*, e5.
40. Haughian, J. M.; Bradford, A. P. *J. Cell. Physiol.* **2009**, *220*, 112.
41. Ou, W.; Zhu, M.; Demetri, G. D.; Fletcher, C. D. M.; Fletcher, J. A. *Oncogene* **2008**, *27*, 5624.
42. Values extracted from the papers related to the PDB codes listed in the Table S1, Supplementary data.
43. Stevens, J. F.; Page, J. E. *Phytochemistry* **2004**, *65*, 1317.